quaternary

MDPI

Article

Between Claudius and Trajan: Palaeoenvironmental Evolution of the Imperial Port of Portus (Central Italy)

Francisco Ruiz [1,2], Gabriel Gómez [1], Javier Bermejo [3], Guadalupe Monge [4,*], María Isabel Carretero [4], María Luz González-Regalado [1], Sergio Ríos [1], Amanda López [3], Alejandro Cano [3], Lucía Fernández [3], Manuel Abad [5], Tatiana Izquierdo [5], Antonio Toscano [1], Paula Gómez [1], José Manuel Bernabé [4] and Verónica Romero [1]

[1] Departamento de Ciencias de la Tierra, Universidad de Huelva, Avda. Tres de Marzo, s/n, 21071 Huelva, Spain; ruizmu@uhu.es (F.R.); gabriel.gomez292@alu.uhu.es (G.G.); montero@dgeo.uhu.es (M.L.G.-R.); riossalgado.sergio@alu.uhu.es (S.R.); antonio.toscano@dgyp.uhu.es (A.T.); paula.gutierrez@alu.uhu.es (P.G.); veronica.romero@dct.uhu.es (V.R.)

[2] Centro de Investigación en Patrimonio Histórico, Cultural y Natural, Campus Universitario de El Carmen, Universidad de Huelva, 21720 Huelva, Spain

[3] Departamento de Historia, Geografía y Antropología, Universidad de Huelva, 21071 Huelva, Spain; javier.bermejo@dhis1.uhu.es (J.B.); amanda.lopez@dhga.uhu.es (A.L.); alejandro.cano1@alu.uhu.es (A.C.); lucia.fernandez@dhga.uhu.es (L.F.)

[4] Departamento de Cristalografía, Mineralogía y Química Agrícola, Facultad de Química, Universidad de Sevilla, Profesor García González nº 1, 41012 Sevilla, Spain; carre@us.es (M.I.C.); jbernabe1@us.es (J.M.B.)

[5] Departamento de Geología, Física y Química Inorgánica, Escuela Superior de Ciencias Experimentales y Tecnología (ESCET), Universidad Rey Juan Carlos, c/Tulipán s/n, 28933 Móstoles, Spain; manuel.abad@urjc.es (M.A.); tatiana.izquierdo@urjc.es (T.I.)

* Correspondence: gmonge@us.es

Abstract

The port of Portus was located about 30 km southwest of Rome and was the most important in the Western Mediterranean during the Roman Imperial period (27 BCE–476 CE). This paper analyses the palaeoenvironmental evolution of the channel linking the outer harbour, or Claudius Basin, with the inner harbour, or Trajan's Hexagon. During the 1st century CE, this area was situated in an open marine environment, which gradually became more confined due to sedimentation from the River Tiber and the silting caused by the massive accumulation of fibres and leaves from the seagrass *Posidonia oceanica*. In the ~2nd–5th centuries CE, the area transitioned to a brackish environment and eventually became silted up, with a marked decline in port activity from the 5th century CE onward.

Keywords: sedimentary facies; macrofauna; microfauna; botany; paleoenvironmental evolution; imperial harbor; central Italy

Check for updates

Academic Editor: Kam-biu Liu

Received: 6 April 2026
Revised: 4 June 2026
Accepted: 18 June 2026
Published: 22 June 2026

Copyright: © 2026 by the authors. Licensee MDPI, Basel, Switzerland. This article is an open access article distributed under the terms and conditions of the Creative Commons Attribution (CC BY) license.

1. Introduction

During the last decades, there has been a proliferation of scientific studies on environmental evolution of marine and estuarine environments throughout the world [1–5]. This research has been based largely on multidisciplinary analysis of surface sections or continuous sediment cores, including textural and mineralogical studies, differentiation of sedimentary facies, definition of the most significant geomorphological structures, the vertical evolution of the fossil or subfossil record, changes in geochemical content or isotopic data, together with the use of radiometric dating [6–8]. The geological record contained in these cores or profiles is the end result of the interaction of eustatic oscillations, climatic changes, regional tectonic-sedimentary evolution, waves, drift currents, river inflows and

human activity, among other factors [9–11]. Knowledge of the geological evolution of a given area is very useful for obtaining information on: (i) ancient marine connections; (ii) the beginning, end or impact of anthropogenic interventions; (iii) changes in palaeoenvironmental conditions; (iv) the refinement of radiometric ages; (v) the detection and impact of high-energy events, such as storms or tsunamis; or (vi) the detection of biotic changes [12,13].

Within the faunal record, various groups have been used as environmental or palaeoenvironmental indicators, such as molluscs [14], foraminifera [15], ostracods [16], calcareous nanoplankton [17] or diatoms [18]. The malacological record of sediments deposited since the last glacial maximum has enabled the reconstruction of sedimentary palaeoenvironments, the inference of sea level changes, the separation of native associations, and the identification of impacts from human activity [19–22]. In these environments, foraminifera and ostracods have also proven to be excellent palaeoenvironmental markers from the last Glacial maximum, with variations in their associations depending on changes in salinity, the palaeogeographic evolution of a given area, metal pollution, sea level changes, or the detection of layers associated with high-energy events [23–27].

The use of all these palaeoenvironmental reconstruction tools is common in archaeological sites, especially within the multidisciplinary analysis of sediment cores. Their main conclusions, together with the data provided by additional surveys, can be used to verify: (i) faunal changes in both space and time [28]; (ii) climatic oscillations [29]; (iii) changes in agricultural plantations in the vicinity of these sites [30]; (iv) ancient diets [31]; or (v) the evolution and decline of harbours [32].

This paper describes and discusses a multiproxy analysis of a continuous core obtained in Portus (Italy), one of the main Mediterranean ports during the Roman imperial era (1st–5th centuries CE). Its objective is to perform a palaeoenvironmental interpretation of the different sedimentary facies based on their textural, macrofaunal, microfaunal and palaeobotanical study, as a basis for inferring their palaeoenvironmental evolution. This study is part of the DEATLANTIR-I and DEATLANTIR-2 projects developed by the University of Huelva in Portus. A summary of the first findings can be consulted in [33].

2. Study Area

The birth of the Roman Empire led to increasingly greater supply needs for the city of Rome. Its status as a metropolis required a constant flow of goods of various types to supply the urban markets. Commercial, economic, and transactional aspects reached their greatest peak in the early 2nd century CE. During this last stage, the territories dominated by Rome reached their maximum extent around 116–117 CE, during the reign of the Spanish emperor Trajan [34]. At that time, Rome was a huge city with more than a million inhabitants, and this enormous population required a controlled system of supplies from the provinces of the Empire, both across the Italian Peninsula and through its ports [35].

This need for a continuous flow of food, combined with a growing population, meant that the ports near Rome were insufficient to meet its needs. As a result, Emperor Claudius ordered the construction of Portus, a new port, around 42 CE, which was later expanded by Emperor Trajan between 100 CE and 112 CE [36]. This port was located about 30 km southwest of Rome, about 3 km north of the ancient port of Ostia and the mouth of the Tiber River. Today, it is part of the Riserva Naturale Statale di Litorale, which borders Leonardo Da Vinci International Airport to the north and the town of Fiumicino to the south.

This very important port consisted of three main elements (Figure 1) [37]: (i) the Claudius basin (~200 ha), which extended westwards into the sea, sheltered by two artificial breakwaters and featuring a central lighthouse [38]; (ii) the dock, a small rectangular basin (~1 ha), to the southwest; and iii) the Trajan basin (32 ha), a hexagon that extended inland

to the east. The connection between Claudius' outer harbour and Trajan's inner hexagon was made via the Canale di Imbocco, bounded to the west by the La Lanterna quay and to the east by the dock [37].

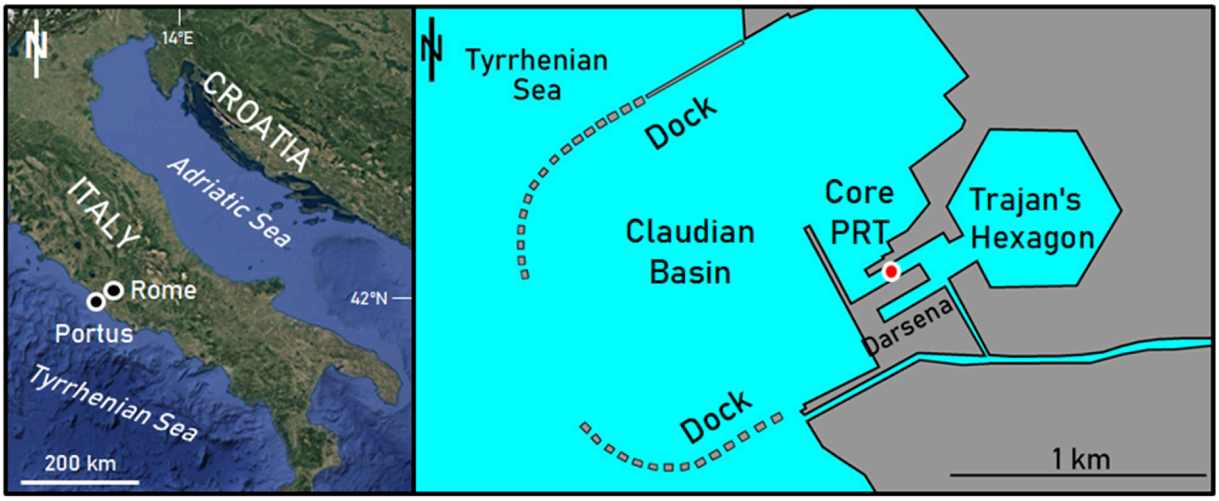

Figure 1. Location and structure of the imperial port of Portus [37]. Grey: port area.

Despite its size, Portus suffered from serious silting problems ever since it was built and was highly exposed to storms from the outset, resulting in the destruction of 200 ships in 63 CE [39]. This necessitated its expansion, as mentioned above, with Trajan's hexagon at the beginning of the 2nd century CE. Between 100 CE and 450 CE, this port was essential both for the export of products from the Tiber valley and for the import of all kinds of raw materials and food from all corners of the Empire. The sacking of Rome by the Vandals (455 CE) and the Gothic Wars (536–552 CE) accelerated its decline [40].

This decline was also caused by the geomorphological changes at the mouth of the River Tiber. During the Empire (1st–5th centuries CE), the coastal areas near Portus remained relatively stable, but a phase of coastal progradation began at the end of this period. This caused the coastline to advance by several hundred metres, leading to the degradation of the port complex, coinciding with the fall of Rome (second half of the 5th century CE). From this date onwards, port activities continued only in the Trajan basin. This progradation stopped during the Medieval Warm Period (~950 CE–1250 CE), but the port was no longer active and was reduced to a swamp. Subsequently, a new intense phase of progradation during the Little Ice Age (~1300 CE–1860 CE) caused the coastline to shift further westward, filling in the Claudius basin and reducing the Trajan basin to a lake [41].

3. Materials and Methods

Core PRT (Figure 2A; 41°46′25″ N; 12°15′12″ E; 5 m depth; 10 cm diameter) was extracted by Geocompany, a drilling company using rotation techniques in the entrance channel to the Trajan basin. In an initial phase, a preliminary visual differentiation of the sedimentary facies was carried out based on their lithology, colour, contact between them, macrofaunal content and visible botanical remains. Eleven samples were separated for a multiproxy study (PRT-1 to PRT-11), taken every 0.5 m vertically. From each sample, 100 g were sieved through screens between 2 mm and 0.063 mm to obtain their granulometric distribution. The residues were dried in an oven at 60 °C for at least two days and served as the basis for the macrofaunal and botanical study.

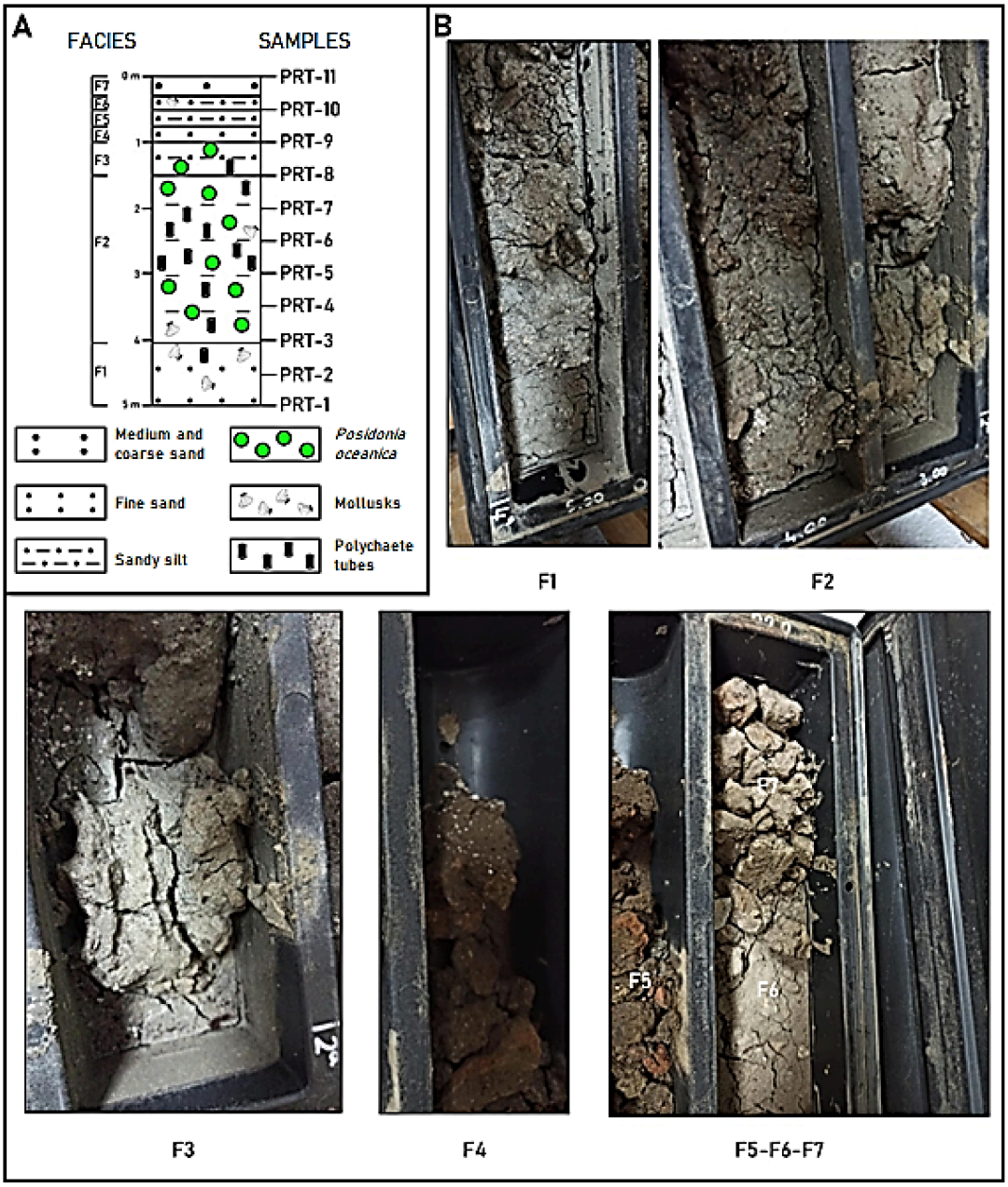

Figure 2. (**A**) Lithostratigraphic column of the PRT core; (**B**) detail of the different sedimentary facies.

All the malacofauna (bivalves, gastropods) present in this waste were extracted and classified according to the keys provided by [42] and the World Register of Marine Species (WoRMS). Specimens of different species of molluscs, as well as other macropalaeontological remains, were photographed with a LEICA binocular magnifying glass connected to a 32" LG television. The abundance of each species in each sample was classified as rare (R: 1–2 specimens), common (C: 3–10 specimens) and abundant (A: more than 10 specimens).

Seven samples (1 g) were selected for micropalaeontological study. The foraminifera present were classified according to [43,44], with updates from the World Foraminifera Database. The distribution of ostracods was also analysed by comparing them with [45–47] and the World Register of Marine Species (WoRMS). The main species of foraminifera and ostracods were photographed using the Scanning Electron Microscope at the Central Research Services of the University of Huelva.

Core PRT is one of a series of cores taken from the Canale di Imbocco during the course of the DEATLANTIR-I and DEATLANTIR-2 projects. One of them (core PT) is located three metres to the east of this core and was studied from a palaeobotanical perspective [48]. The radiocarbon dates of two samples taken from the PT core can therefore be extrapolated laterally to the PRT core (Table 1; 5–4.9 m depth: 75 BCE–190 CE; 1.9–1.8 m depth: 217 CE–465 CE), with the most probable ages towards the second half of the 1st century CE and the 4th century CE, respectively.

Table 1. Radiocarbon dates of core PT. Original data from [48], now calibrated with Calib 8.2.

Depth (m)	Material	Laboratory Number	Uncalibrated C^{14} Age (BP)	Error	Calibrated C^{14} Age (BCE/CE)	Median Probability
1.8–1.9	*Cerastoderma glaucum*	Beta-602823	2250	30	217 CE–465 CE	339 CE
4.9–5	*Polititapes rhomboides*	Beta-602826	2480	30	75 BCE–190 CE	52 CE

4. Results

4.1. Sedimentary Facies and Macrofauna

Seven sedimentary facies have been differentiated in the PRT core (Figure 2B). F1 (5–4.1 m) consists of finely compacted sands with numerous bioclasts (bioclastic gravel: 30.6–58.8%; sand: 28.5–53%; silt + clay: 12.7–16.4%). Bivalves are represented by *Eastonia rugosa* (Helbling, 1779), *Ruditapes decussatus* (Linnaeus, 1758) and fragments of *Acanthocardia* sp. (Table 2). Specimens of the gastropod *Pisania striata* (Gmelin, 1791) have also been extracted, as well as barnacle plates and some calcareous tubes of polychaete annelids. The grey mud of F2 (4.1–1.5 m; bioclastic gravel: 3.2–29.2%; sand: 14.1–34.5%; silt + clay: 51.4–79.6%) contains abundant fibres from the marine phanerogam *Posidonia oceanica* (Linnaeus) Delile, 1813, as well as numerous polychaete tubes between 3 m and 2.5 m deep. The most representative mollusks are the bivalves *Mytilus galloprovincialis* Lamarck, 1819 and *Cerastoderma edule* (Linnaeus, 1758), together with the gastropod *Tritia corniculum* (Olivi, 1792).

Table 2. Macrofaunal record of core PRT. R: rare; F: frequent; A: abundant.

GROUP/SPECIES	Samples (PRT–)	1	2	3	4	5	6	7	8	9	10	11
	Depth (m)	5	4.5	4	3.5	3	2.5	2	1.5	1	0.5	0.2
	Facies	F1	F1	F2	F2	F2	F2	F2	F3	F4	F6	F7
BIVALVES	*Acanthocardia* sp.		R									
	Cerastoderma edule (Linnaeus, 1758)					R	R	R				
	Eastonia rugosa (Helbing, 1779)	R	R	R								
	Mytilus galloprovincialis Lamarck, 1819						R	R			R	
	Mytilus sp.			R								
	Ruditapes decussatus (Linnaeus, 1758)		R									
	Family Veneridae									R		
GASTROPODS	*Charpentieira itala* (von Martens, 1824)								R			
	Pisania striata (Gmelin, 1791)			R								
	Tritia corniculum (Olivi, 1792)											
OTHER GROUPS	Tubes of polychaete annelids		R	R	R	F	A	F	R			
	Cirriped crustacean plates		R				R					
	Posidonia oceanica fibres				F	F	A	F	R	R		

F3 (1.5–1 m) consists of sandy silts (bioclastic gravel: 3.2%; sand: 17.2%; silt + clay: 79.6%) rich in *Posidonia oceanica* fibres and some polychaete tubes. No bivalve remains have been observed, and only isolated specimens of the terrestrial gastropod *Charpentieira itala*

(von Martens, 1824) have been extracted. This facies includes numerous lithic fragments and remains of construction materials. F4 (1–0.75 m) is characterised by the presence of sandy silts with numerous carbonate clasts and volcanic rock fragments (carbonate gravel: 24.6%; sand: 28%; silt + clay: 47.4%). Only a few fragments of bivalves belonging to the Veneridae family have been identified in this facies.

F5 (0.75–0.55 m) comprises brown sandy silts with a significant number of microconglomerates and some scattered plant fragments, while F6 (0.55–0.35 m) is composed of clayey silts (gravel: 2.7%; sand: 17.4%; silt + clay: 79.9%) with carbonate remains and lithic fragments, ceramic and construction material and highly fragmented valves of the bivalve *Mytilus galloprovincialis*. The upper 35 cm of the PRT core (F7) consists of medium-coarse sand and conglomerates (gravel + conglomerate: 71.2%; sand: 16.3%; clay:12.5%) with abundant remains of construction materials (mortar, volcanic rock fragments).

4.2. Microfauna

Foraminifera are very scarce in the PRT core samples (Table 3). A total of 43 individuals belonging to 16 species have been identified, of which 15 are benthic and *Trilobatus trilobus* (Reuss, 1859) is planktonic. In relation to their distribution, the following characteristics can be highlighted: (i) their absence in PRT-1, PRT-10 and PRT-11; (ii) the predominance of marine species (e.g., *Bolivina*, *Cassidulina*, *Cibicides*, *Cibicidoides*, miliolids) over species more typical of restricted and euryhaline environments [*Ammonia tepida* (Cushman, 1826), *Haynesina* spp.] between 4 m and 2 m depth; and (iii) the dominance of the latter, as well as agglutinated forms typical of marshes [e.g., *Trochammina inflata* (Montagu, 1808)] at 1 m depth.

A total of 47 ostracod valves belonging to 15 species have been extracted, three of which have been left in open nomenclature due to breakage or because they are juvenile specimens (Table 2). These microcrustaceans have not been observed in PRT-1, PRT-10 and PRT-11, while they reach their maximum diversity (9 species) and abundance (15 specimens) in sample PRT-7 (2 m depth). This sample and PRT-3 (4 m depth) coincide in the presence of *Leptocythere castanea* (Sars, 1866), *Palmoconcha agilis* (Ruggieri, 1967) and *Pontocythere turbida* (Müller, 1894), while PRT-9 (1 m depth) is dominated by smooth specimens of *Cyprideis torosa* (Jones, 1850) and *Loxoconcha elliptica* Brady, 1868).

Table 3. Microfaunal record of core PRT.

GROUP/SPECIES	Samples (PRT–)	1	3	5	7	9	10	11
	Depth (m)	5	4	3	2	1	0.5	0.2
	Facies	F1	F2	F2	F2	F4	F6	F7
FORAMINIFERA	*Ammonia beccarii* (Linnaeus, 1758)					1		
	Ammonia tepida (Cushman, 1926)			3		5		
	Bolivina punctata D'Orbigny, 1839				1			
	Bolivina spathulata (Williamson, 1858)				2			
	Cassidulina laevigata D'Orbigny, 1826				1			
	Cibicides refulgens Montford, 1808				1			
	Cibicidoides pseudoungerianus Cushman, 1922				2			
	Elphidium advenum (Cushman, 1922)		1					
	Haynesina depressula (Ehrenberg, 1840)		2			2		
	Haynesina germanica (Walker & Jacob, 1796)		1			1		
	Pleurostomella acuminata Cushman, 1922			1				
	Quinqueloculina seminulum (Linnaeus, 1758)				5			
	Rosalina globularis D'Orbigny, 1826				1			
	Triloculina oblonga (Montagu, 1803)		2	2	5			
	Trochammina inflata (Montagu,1808)					2		
	Trilobatus trilobus (Reuss, 1850) -Planktonic-	1				1		

Table 3. *Cont.*

OSTRACODS	*Bairdia longivaginata* (Müller, 1894)					1		
	Cyprideis torosa (Jones, 1850)					15		
	Cytheropteron sp.					1		
	Eucytherura sp.		1					
	Heterocypris salina (Brady, 1868)					1		
	Leptocythere castanea (Sars, 1866)		3		1			
	Leptocythere sp.				1			
	Loxoconcha elliptica Brady, 1868		1			5		
	Loxoconcha rhomboidea (Fisher, 1855)				1			
	Palmoconcha agilis (Ruggieri, 1867)		1		2			
	Pontocypris acuminata (Ath, 1850)				4			
	Pontocythere turbida (Müller, 1894)		3		2			
	Triebelina raripila (Müller, 1894)				1			
	Xestoleberis communis (Müller, 1894)				2			
	Xestoleberis plana (Müller, 1894)			1				

5. Discussion

5.1. Autoecology of the Main Species

5.1.1. Bivalves

Mytilus galloprovincialis Lamarck, 1819 (Figure 3A), also known as the Mediterranean mussel, is a sessile bivalve typical of hard substrates (e.g., rocky coasts, pier jetties), to which it attaches itself by means of a byssus [49]. It is a species found in marine environments, where it has a high tolerance to environmental variations, withstanding temperatures between 7 °C and 24 °C as well as episodes of desiccation [50]. *Cerastoderma edule* (Linnaeus, 1758) (Figure 3C), commonly known as the common cockle, is a species that usually lives in the infralittoral zone, on both sandy and muddy substrates, as well as on estuary beaches. It is a euryhaline species that can tolerate salinities of up to $5^0/_{00}$. It is found from Norway to the east coast of Africa, as well as in the Mediterranean [51,52].

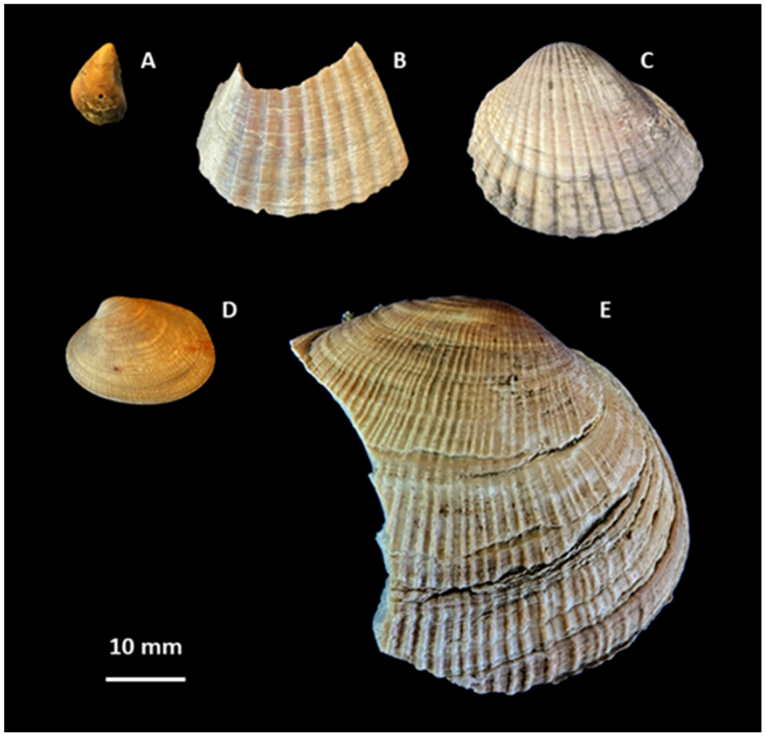

Figure 3. Bivalves. (**A**) *Mytilus galliprovincialis*; (**B**) *Acanthocardia* sp.; (**C**) *Cerastoderma edule*; (**D**) *Ruditapes decussatus*; (**E**) *Eastonia rugosa*.

Ruditapes decussatus (Linnaeus, 1758) (Figure 3D) is a marine species found along the Atlantic coasts of Europe and as far south as Senegal, as well as in the Mediterranean [53]. This infaunal species is common in sandy and silty-sandy sediments, from the intertidal zone to depths of 5 m in bays, estuaries and coastal lagoons [54–56]. *Eastonia rugosa* (Helbling, 1779) (Figure 3E) is a marine bivalve that lives on soft sublittoral substrates. The influence of fresh water is not an obstacle to its development and it can be found in river deltas [57,58].

5.1.2. Gastropods

Tritia corniculum (Olivi, 1792) (Figure 4A) is a marine species originally native to the Mediterranean that has spread as far as the Bay of Biscay. It has been described as a scavenger [59]. *Pisania striata* (Gmelin, 1791) (Figure 4B) is a marine species that has been described in Mediterranean coastal environments [60]. It usually lives in intertidal zones, where it mainly preys on bivalves [61]. *Charpentiera ítala* (von Martens, 1824) (Figure 4C) is a terrestrial gastropod that has been described in the Rhône River [62]. There is little information available on this species.

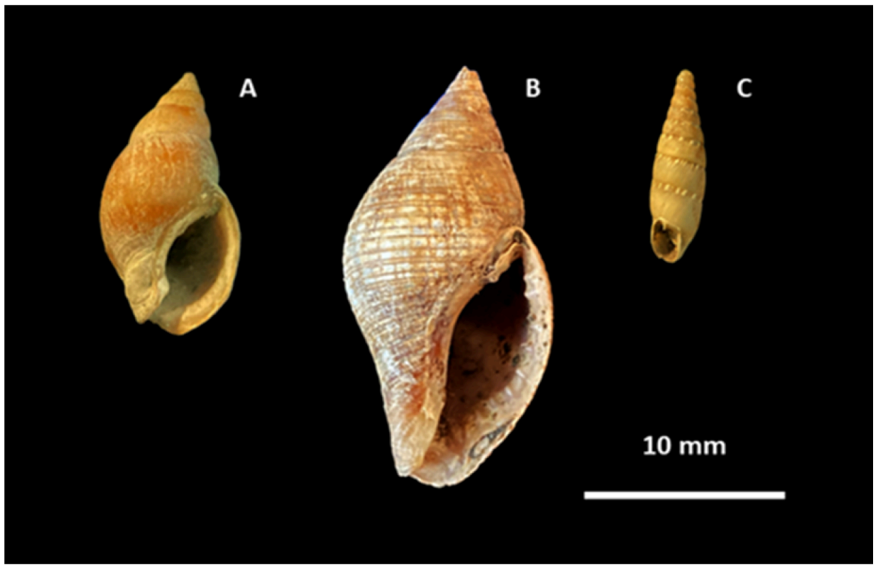

Figure 4. Gastropods. (**A**) *Tritia corniculum*; (**B**) *Pisania striata*; (**C**) *Charpenteira itala*.

5.1.3. The Endemic Seagrass *Posidonia oceanica*

Leaves and fibres from this marine phanerogam make up a substantial part of F2 (Figure 5). It forms extensive meadows in shallow coastal areas (<40 m depth) of the Mediterranean, where it currently occupies 1.2 million hectares [63].

Figure 5. Fibres of *Posidonia oceánica*.

5.1.4. Foraminifera

Ammonia tepida (Cushman, 1926) (Figure 6A,B) has been frequently described in coastal lagoons, subtidal areas of channels located in the middle and upper parts of estuaries, deltas or rias. It is a euryhaline species and is usually associated with bottoms rich in organic matter with restricted tidal circulation [64,65]. *Haynesina depressula* (Walker & Jacob, 1798) (Figure 6C) is also typical of this type of coastal environment, especially those with significant variations in salinity. This species can live on substrates of varying grain size [66,67].

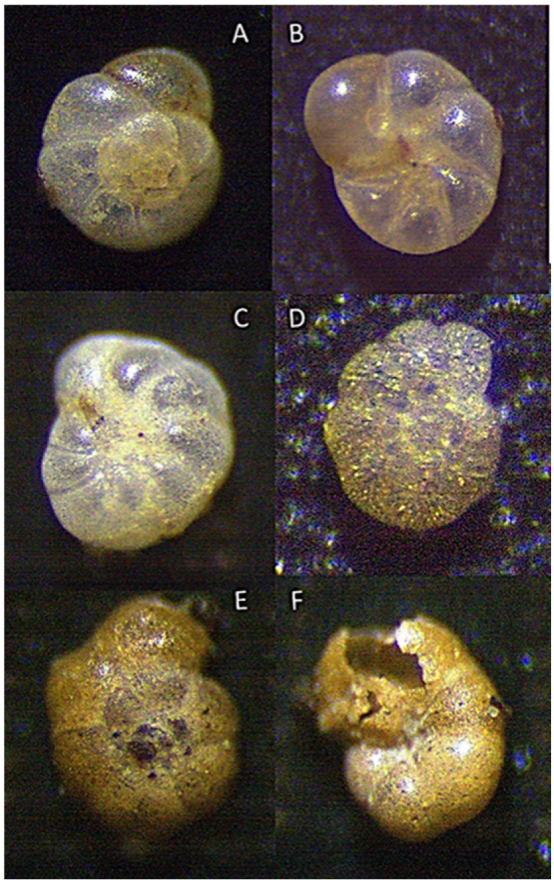

Figure 6. Foraminifera. (**A**,**B**) *Ammonia tepida*; (**C**) *Haynesina depressula*; (**D**) *Haynesina germánica*; (**E**,**F**) *Trochammina inflata*.

5.1.5. Ostracods

Cyprideis torosa (Jones, 1850) (Figure 7A) is the most abundant ostracod species in the PRT sample. It is a species typical of coastal lagoons, estuaries, deltas, and marshes, where it has been found in a wide range of salinities, although its optimal range is between $2^{0}/_{00}$ and $16.5^{0}/_{00}$ [46,68]. *Loxoconcha elliptica* Brady, 1868 (Figure 7B) is commonly found in tidal channels and marshes in numerous estuaries and coastal areas in Europe. It usually tolerates significant changes in salinity and tends to prefer silty-clay substrates [69,70]. Other species, such as *Bairdia longivaginata* Müller, 1894, *Palmoconcha agilis* (Ruggieri, 1967), *Pontocythere turbida* (Müller, 1894) and *Triebelina raripila* (Mueller, 1894), are typical of coastal environments on the Italian peninsula [45,71].

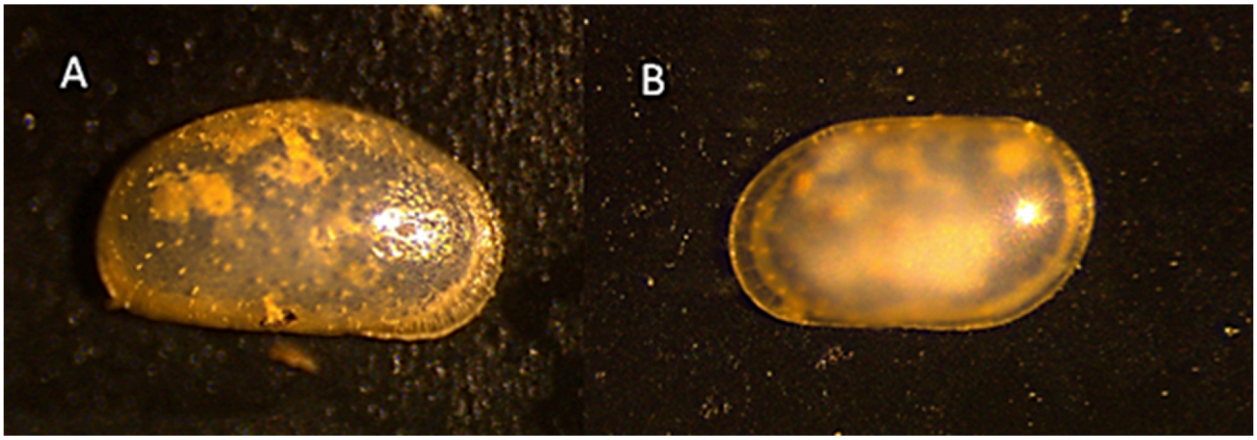

Figure 7. Ostracods. (**A**) *Cyprideis torosa*; (**B**) *Loxoconcha elliptica*.

5.2. Between Claudius and Trajan: A Palaeoenvironmental Reconstruction

The distribution of sedimentary facies and the faunal and botanical record, as well as comparison with the radiocarbon dating of a nearby core, allows us to differentiate four phases in the palaeoenvironmental reconstruction of the Canale di Imbocco:

Phase 1 (~1st century CE). This corresponds to the FA-1 deposit (5–4.1 m), whose scarce fauna is entirely marine in origin (*Eastonia*, *Ruditapes*) and would identify sediment transport from the adjacent inner shelf or from nearby beaches located west of Portus [72]. In addition, numerous seeds of intertidal or subtidal phanerogams appear together with these marine species in the adjacent PT core, most likely dating to the first century CE [48] (see Table 1). This interpretation would coincide with historical data, which point to the silting problems experienced by Portus [47] and which subsequently led to the construction of Trajan's hexagon.

Phase 2 (~2nd–5th centuries CE). The transition to FA-2 represents a notable change in sedimentation, as well as in the faunal and botanical record. There is a significant decrease in grain size and a massive deposit of *Posidonia oceanica* fibres, which would cause siltation problems in this port [73]. The microfauna reflects a mixture of euryhaline species (*Haynesina*, *Leptocythere*) together with a large group of marine species in all the groups studied. This facies is interpreted as the main fill of the Canale di Imbocco since the construction of Trajan's pier, in a hydrodynamically calm environment with variable salinity due to the mixing of contributions from the River Tiber and the tides. This facies has also been observed at the PT core up until the 5th century CE [48] (Table 1). The occasional increase in marine fauna could correspond to periodic dredging of this channel, which would increase tidal flow, storms or high tides.

Phase 3 (5th century CE). The transition between FA-2 and FA-3 represents a notable change in environmental conditions, with the presence of both euryhaline species (*Cyprideis*, *Loxoconcha*) and marsh species (e.g., *Trochammina*) and even freshwater species (*Heterocypris*), as well as the almost total disappearance of *Posidonia* fibres. This would imply a drastic reduction in tidal flows and the almost total obstruction of the marine connection, which was completed around the 5th century CE [74].

Phase 4 (after the 5th century CE). This phase would include FA-4 to FA-7 and would involve the progressive filling of the Canale di Imbocco with materials of mainly anthropogenic origin, such as remains of construction elements, fragments of volcanic rocks used for the construction of Portus, and ceramic remains, as noted at the top of the PT core [48]. The scarce fauna, consisting mainly of juvenile mussels, could come from complete specimens of this family that lived sessile in internal areas of the ancient port facilities.

6. Conclusions

1. The multidisciplinary study of a core obtained in transit between the outer harbour of Claudius and the inner hexagon of Trajan, the two most important areas of the imperial Roman port of Portus, has enabled an assessment of the palaeoenvironmental changes that took place between the 1st century CE and the centuries following the 5th century CE at this archaeological site.
2. Seven sedimentary facies have been differentiated based on their texture, macrofauna, microfauna and botanical remains (mainly *Posidonia oceanica* fibres).
3. The fauna record consists of seven species of bivalves, three species of gastropods, 16 species of foraminifera and 15 species of ostracods, as well as remains of barnacles and serpulids.
4. The botanical record is very important in some facies, where fibres and leaves of *Posidonia oceanica* constitute a significant percentage. This phanerogam would cause silting problems in this channel.
5. The inferred palaeoenvironmental evolution of the channel linking the outer Claudio basin and the inner Trajan hexagon would indicate a transition from a relatively open marine environment, probably prior to the construction of Trajan's hexagon, to a channel with a mixture of marine and river waters that would contain an abundant record of *Posidonia* on its bottom, ending with progressive silting, loss of tidal influence and final anthropogenic filling.

Author Contributions: Conceptualization, F.R., J.B., G.G., G.M. and S.R.; methodology, F.R.; software, F.R., S.R., M.A. and T.I.; validation, F.R. and J.B.; formal analysis, F.R., G.G., G.M. and J.B.; investigation, all authors; resources, F.R., J.B., G.M. and M.I.C.; data curation, F.R., S.R. and M.A.; writing—original draft preparation, all authors; writing—review and editing, all authors; visualization, F.R.; supervision, J.B. and M.I.C.; project administration, F.R. and J.B.; funding acquisition, J.B. All authors have read and agreed to the published version of the manuscript.

Funding: This study was supported by the following projects: (1) Proyecto del Plan Operativo FEDER 2021-2027 Arqueología y Virtualización: nuevas técnicas de teledetección y digitalización aplicadas al patrimonio arqueológico (ARQUEOVIRT) Ref. EPIT1622023; Mors et funus ostiense: ritual, arquitectura y topografía portuaria en Ostia Antica y Portus del periodo altoimperial a la tardoantigüedad Proyectos Arqueológicos en el Exterior Ministerio de Cultura; (2) project FEDER 2014-2020 UHU-1260298, and (3) project "El arco atlántico del sudoeste hispano desde la protohistoria hasta la Tardoantiguedad: Evolución geomorfológica, ocupación litoral y sistemas portuarios" (Ref. PID2022-142778NB-I00) Proyectos Generación del conocimiento convocatoria 2022. Other funds come from the research groups HUM-132, RNM-238 and RNM-293 of the University of Huelva and RNM-349 of the University of Sevilla. It is a contribution to the Center for Research in Historical, Cultural and Natural Heritage of the University of Huelva. The paleontological record is deposited in the Paleontology and Applied Ecology Laboratory of the University of Huelva.

Data Availability Statement: The original contributions presented in this study are included in the article. Further inquiries can be directed to the corresponding author.

Acknowledgments: This article is dedicated to Adolfo Francisco Muñoz, who passed away recently and who studied the palaeobotany of Portus with great dedication.

Conflicts of Interest: The authors declare no conflicts of interest.

References

1. Espinosa, M.; De Francesco, C.; Isla, F. Paleoenvironmental reconstruction of Holocene coastal deposits from the Southeastern Buenos Aires Province, Argentina. *J. Paleolimnol.* **2003**, *29*, 49–60. [CrossRef]
2. Allison, A.J.; Niemi, T.M. Paleoenvironmental reconstruction of Holocene coastal sediments adjacent to archaeological ruins in Aqaba, Jordan. *Geoarchaeology* **2010**, *25*, 602–625. [CrossRef]

3. Székely, S.-F.; Bindiu-Haitonic, R.; Filipescu, S.; Bercea, R. Biostratigraphy and paleoenvironmental reconstruction of the marine lower Miocene Chechiș Formation in the Transylvanian Basin based on foraminiferal assemblages. *Carnets Geol.* **2017**, *17*, 11–37. [CrossRef]
4. Pereira, A.; Laprida, C.; Fucks, E. Paleoenvironmental reconstruction of the pleistocene regressive marine successions from Salado Basin, northeastern Buenos Aires (Argentina). *J. S. Am. Earth Sci.* **2022**, *118*, 103906. [CrossRef]
5. Fu, G.; Chen, W.; Wu, S.; Wang, S.; Chen, J.; Zeng, F.; Sun, Y.; Li, X. Stratigraphic sequences off NE Hainan Island: Controls on sand resource distribution in the South China Sea. *Reg. Stud. Mar. Sci.* **2025**, *89*, 104327. [CrossRef]
6. Badejo, A.O.; Choi, B.-H.; Cho, H.-G.; Yi, H.-I.; Shin, K.-H. A paleoenvironmental reconstruction of the last 15,000 cal yr BP via Yellow Sea sediments using biomarkers and isotopic composition of organic matter. *Clim. Past Discuss.* **2014**, *10*, 1527–1565.
7. Pelage, L.; González, J.G.; Leloch, F.; Ferreira, V.; Munaron, J.-M.; Lucena-Frédou, F.; Frédou, T. Importance of estuary morphology for ecological connectivity with their adjacent coast: A case study in Brazilian tropical estuaries. *Estuar. Coast. Shelf Sci.* **2021**, *251*, 107184. [CrossRef]
8. Irabien, M.J.; Cearreta, A.; Gómez-Arozamena, J.; García-Artola, A.; Serrano-García, H.; Gardoki, J. Tracing pollution legacies in the Suances Estuary (N Spain): Challenges for dating methods and ecological recovery after mine closure. *Reg. Stud. Mar. Sci.* **2025**, *91*, 104511. [CrossRef]
9. Costa, A.M.; Freitas, M.C.; Leira, M.; Fonseca, R.; Duarte, J.; Diniz, M.; Arias, P. Late Holocene evolution of a Mediterranean incised river flowing to the Atlantic: Sedimentary dynamics, fluvial activity and paleoenvironmental reconstruction (SW Iberia). *Quat. Int.* **2022**, *638–639*, 37–55. [CrossRef]
10. Crow, J.M. Searching the ocean for secrets to help fight climate change. *Nature* **2023**, *514*, 686.
11. Utami, D.A.; Solihuddin, T.; Sibert, E.C.; Cohen, A.; Cahyarini, S.Y. Vertical profiles of microplastics in coastal sediments of Panjang Island, Java Sea. *Reg. Stud. Mar. Sci.* **2025**, *91*, 104518. [CrossRef]
12. Andrews, J.T.; Helgadóttir, G. Late Quaternary Ice Cap Extent and Deglaciation, Húnaflóaáll, Northwest Iceland: Evidence from Marine Cores. *Arct. Antarct. Alp. Res.* **2003**, *35*, 218–232. [CrossRef]
13. Tsujimoto, A. Changes in deep-sea benthic foraminiferal fauna caused by turbidites de-posited after the 2011 Tohoku-oki earthquake. *Mar. Geol.* **2020**, *419*, 106045. [CrossRef]
14. Al-Ameri, I.D.S.; Briant, R.M. A late Holocene molluscan-based palaeoenvironmental reconstruction from southern Mesopotamia: Implications for the palaeogeographic evolution of the Arabo-Persian Gulf. *J. Afr. Earth Sci.* **2019**, *152*, 1–9. [CrossRef]
15. Rojas-Portilla, L.; Ochoa, D.; Cardich, J.; Silva-Berrospi, E.; Cárdenas-Farfán, S.; Aguirre-Velarde, A.; Carré, M.; Djouraev, I.; Hidalgo, S.; Gutiérrez, D.; et al. Heavy metal accumulation and benthic foraminiferal response following the Peruvian Ventanilla crude oil spill (January 2022). *Reg. Stud. Mar. Sci.* **2025**, *90*, 104459. [CrossRef]
16. Sasaki, S.; Irizuki, T.; Seto, K.; Suganuma, Y. Ostracoda and Paleoenvironment of Holocene-Raised Beach Sediment in Skarvsnes, East Antarctica. *Paleontol. Res.* **2022**, *26*, 440–454. [CrossRef]
17. Ion, G.; Briceag, A.; Vasiliu, D.; Lupascu, N.; Melinte-Dobrinescu, M. A multiproxy reconstruction of the Late Pleistocene-Holocene paleoenvironment: New insights from the NW Black Sea. *Mar. Geol.* **2022**, *443*, 106648. [CrossRef]
18. Espinosa, M.; Fayó, R.; Vélez-Agudelo, C. Diatom-based paleoenvironmental reconstruction from the coast of Northern Patagonia, Argentina. *J. S. Am. Earth Sci.* **2022**, *116*, 103874. [CrossRef]
19. Schnedl, S.M.; Haselmair, A.; Gallmetzer, I.; Mautner, A.K.; Tomašových, A.; Zuschin, M. Molluscan benthic communities at Brijuni Islands (northern Adriatic Sea) shaped by Holocene sea-level rise and recent human eutrophication and pollution. *Holocene* **2018**, *28*, 1801–1817. [CrossRef] [PubMed]
20. Rao, K.N.; Pandey, S.; Kubo, S.; Saito, Y.; Kumar, K.C.V.; Demudu, G.; Malini, B.H.; Na-gumo, N.; Nakashima, R.; Sadakta, N. Paleoclimate and Holocene relative sea-level his-tory of the east coast of India. *J. Paleolimnol.* **2020**, *64*, 71–89. [CrossRef]
21. Noti, A.; Lourens, L.J.; Geraga, M.; Wesselinngh, F.P.; Haghipour, N.; Georgiou, N.; Christodoulou, D.; Sergiou, S.; Dimas, X.; Vlachapoulos, A.G.; et al. Holocene Paleoenvironmental Evolution of a Semi-Enclosed Shallow Aegean Basin: A Combination of Seismic Stratigraphy and Sediment Core Proxies. *Water* **2022**, *14*, 3688. [CrossRef]
22. De Falco, G.; Carannante, A.; Del Vais, C.; Gasperini, L.; Sanna, I.; Cammarano, F.; Cozzolino, M.; Pascussi, V.; Conforti, A. Late Holocene Evolution of the Lagoonal Harbour of the Punic Centre of Othoca (Western Sardinia, Mediterranean Sea). *Geoarchaeology* **2025**, *40*, e70010. [CrossRef]
23. Triantaphyllou, M.V.; Tsourou, T.; Kouli, K.; Koukousioura, O.; Dimiza, M.D.; Aidona, E.V.; Syrides, G.; Antoniou, V.; Panagiotopoulos, I.P.; Vandarakis, D.; et al. Paleoenvironmental Evolution and Sea Level Change in Saronikos Gulf (Aegean Sea, Greece): Evidence from the Piraeus Coastal Plain and Elefsis Bay Sedimentary Records. *Water* **2021**, *13*, 1621. [CrossRef]
24. Fouet, M.P.A.; Singer, D.; Coynel, A.; Héliot, S.; Howa, H.; Lalande, J.; Mouret, A.; Schweizer, M.; Tcherkez, G.; Jorissen, F.J. Foraminiferal Distribution in Two Estuarine Intertidal Mudflats of the French Atlantic Coast: Testing the Marine Influence Index. *Water* **2022**, *14*, 645. [CrossRef]

25. Duan, B.; Li, T.; Wang, L.; Xiong, Z. Holocene sea level change and paleoenvironmental evolution off the Shandong Peninsula: Evidence of benthic foraminifera assemblages from core LHSD-1 in a subaqueous clinoform. *J. Sea Res.* **2023**, *192*, 102338. [CrossRef]
26. Chitnarin, A.; Forel, M.-B.; Tepnarong, P. Holocene ostracods (Crustacea) from a whale-fall excavation site from the Chao Phraya delta, Central Thailand. *Eur. J. Taxon.* **2023**, *856*, 120–151. [CrossRef]
27. Stoltenberg, M.R.; Junna, T.; Davies, J.; Kristensen, K.; Hansen, K.E.; Pearce, C.; Seidenkrantz, M.-S. Time-transgressive response of benthic foraminifera to the deglaciation of the Northeast Greenland shelf. *Quat. Sci. Rev.* **2025**, *362*, 109407. [CrossRef]
28. Antczak-Orlewska, O.; Okupny, D.; Kruk, A.; Bailey, R.I.; Plöciennik, M.; Sikora, J.; Krapied, M.; Kittel, M.; Kittel, P. The spatial and temporal reconstruction of a medieval moat ecosystem. *Sci. Rep.* **2022**, *12*, 20679. [CrossRef] [PubMed]
29. Sandweiis, H.; Andrus, F.T.; Kelley, A.R.; Roscoe, P.B. Archaeological climate proxies and the complexities of reconstructing Holocene El Niño in coastal Peru. *Proc. Natl. Acad. Sci. USA* **2020**, *117*, 8271–8279. [CrossRef] [PubMed]
30. Farley, G.; Schneider, L.; Clark, G.; Haberle, S.G. A Late Holocene palaeoenvironmental reconstruction of Ulong Island, Palau, from starch grain, charcoal, and geochemistry analyses. *J. Archaeol. Sci. Rep.* **2018**, *22*, 248–256. [CrossRef]
31. Rivals, F.; Cohen, J.; Desclaux, E. Dietary traits of the ungulates from the Middle Pleistocene sequence of Lazaret Cave: Palaeoecological and archaeological implications. *Archaeol. Anthropol. Sci.* **2023**, *15*, 23. [CrossRef]
32. Melis, R.; Borgia, E.; Agostini, S.; Celant, A.; Di Rita, F.; Forte, E.; Salvi, G.; Colizza, E. Palaeoenvironmental evolution and decline of the harbours of the Roman and Early Byzantine city of Elaiussa Sebaste (southeastern Turkey): Natural and anthropic causes. *J. Quat. Sci.* **2025**, *40*, 153–173.
33. Bermejo, J.; Campos, J.M.; Sebastiani, R.; Fernández, L.; Bermejo, A.; Marfil, F.; D'Amassa, C.; Baena, F.; Domínguez, E.; Rodríguez, N.E.; et al. Los puertos imperiales de Roma: Investigaciones geoarqueológicas en el muelle este-oeste de Portus. In *Del Atlántico al Tirreno. Puertos Hispanos e Itálicos*; Campos, J.M., Smith, R.Z., Eds.; Editorial Universidad de Huelva: Huelva, Spain, 2021; pp. 582–610.
34. Garnsey, P.; Saller, R. *El Imperio Romano. Economía, Sociedad y Cultura*; Editorial Crítica: Barcelona, Spain, 1991.
35. Roda, I. Ayer Roma, hoy nosotros. In *El legado Romano: Historia, Cultura y Patrimonio*; Lorenzana, F., Mateos, F., Coords, Eds.; Sociedad Extremeña de Historia: Llerena, Spain, 2023; pp. 33–43.
36. Pepe, C.; Giardini, M.; Giraudi, C.; Masi, A.; Mazzini, I.; Sadori, L. Plant landscape and environmental changes recorded in marginal marine environments: The ancien Roman harbour of Portus (Rome, Italy). *Quat. Int.* **2013**, *303*, 73–81. [CrossRef]
37. Keay, S. The port system of Imperial Rome. *Archaeol. Monog. Br. Sch. Rome* **2012**, *21*, 33–67.
38. Goiran, J.-P.; Salomon, F.; Mazzini, I.; Bravard, J.-P.; Pleuger, E.; Vittori, C.; Boetto, G.; Cristiansen, J.; Arnaud, P.; Pellegrino, A.; et al. Geoarchaeology confirms location of the ancient harbour basin of Ostia (Italy). *J. Archaeol. Sci.* **2014**, *41*, 389–398. [CrossRef]
39. Tacitus. *Annales*; Collection Des Universités de France; Les Belles Lettres: Paris, France, 2010.
40. O'Connell, T.C.; Ballantyne, R.M.; Hamilto-Dyer, S.; Margaritis, E.; Oxford, S.; Pantano, W.; Millett, M.; Keay, S.J. Living and dying at the Portus Romae. *Antiquity* **2019**, *93*, 719–734. [CrossRef]
41. Di Bella, L.; Bellotti, P.; Frezza, V.; Bergamin, L.; Carboni, M.G. Benthic foraminiferal assemblages of the imperial harbor of Claudius (Rome): Further paleoenvironmental and geoarcheological evidences. *Holocene* **2011**, *21*, 1245–1259. [CrossRef]
42. Trainito, E.; Doneddu, M. *Conchiglie del Mediterraneo*; Il Castello: Milán, Italy, 2005.
43. Hayward, B.W.; Le Coze, F.; Vachard, D.; Gross, O. World Foraminifera Database. Available online: https://www.marinespecies.org/foraminifera/index.php (accessed on 21 May 2025).
44. Milker, Y.; Schmiedl, G. A taxonomic guide to modern benthic shelf foraminifera of the western Mediterranean Sea. *Palaeont. Elect.* **2012**, *15*, 1–134. [CrossRef]
45. Bonaduce, G.; Ciampo, G.; Masoli, M. Distribution of Ostracoda in the Adriatic Sea. *Pubbl. Staz. Zool. Napoli* **1976**, *40*, 372–428.
46. Meisch, C. *Freshwater Ostracods of Western and Central Europe*; Spektrum Akad-Emischer Verlag GmbH: Heidelberg/Berlin, Germany, 2000.
47. Mazzini, I.; Faranda, C.; Giardini, C.; Giraudi, C.; Sadori, I. Late Holocene palaeoenvironmental evolution of the Roman harbour of Portus, Italy. *J. Paleolimnol.* **2011**, *46*, 243–256. [CrossRef]
48. Muñoz, A.F.; Ruiz, F.; Campos, J.M.; Bermejo, J.; Fernández, L.; Bermejo, A.; Rodríguez Vidal, J.; Gómez, G.; González-Regalado, M.L.; Cáceres, L.M.; et al. Late Holocene archaeobotanical evolution of the Canale di Imbocco (Roman imperial port of Portus, Central Italy). *Rev. Palaeobot. Palinol.* **2022**, *302*, 104670. [CrossRef]
49. Trozic-Borovac, S.; Icanovic, J.; Imamovic, A.; Bijedic, A.; Celebicic, M. Phenotypic characteristics of mussel *Mytilus galloprovincialis* Lamarck, 1873 in the Neum Bay (Bosnia and Herzegovina). *Veterinaria* **2022**, *71*, 205–218. [CrossRef]
50. Anestis, A.; Lazou, A.; Portner, H.O.; Michaelidis, B. Behavioral and metabolic, and molecular stress responses of marine bivalve *Mytilus galloprovincialis* during long-term acclimation at increasing ambient temperature. *Am. J. Physiol.-Regul. Integr. Compar. Physiol.* **2007**, *293*, R911–R921. [CrossRef] [PubMed]
51. Pérez Camacho, A.; Román, G. Crecimiento, reproducción, mortalidad y producción del berberecho *Cerastoderma edule* (L.) en la Ría de Arosa. *Cuad. Area Cienc. Mar.* **1984**, *1*, 499–507.

52. Available online: www.asturnatura.com (accessed on 25 May 2025).
53. Breber, P. On-growing of the carpet-shell clam (*Tapes decussatus* (L.)): Two years' experience in Venice Lagoon. *Aquaculture* **1985**, *44*, 51–56. [CrossRef]
54. Bebianno, M.J.; Géret, F.; Hoarau, P.; Serafim, M.A.; Coelho, M.R.; Gnassia-Barelli, M.; Roméo, M. Biomarkers in *Ruditapes decussatus*: A potential bioindicator species. *Biomarkers* **2004**, *9*, 305–330. [CrossRef] [PubMed]
55. Juanes, J.A.; Bidegain, G.; Echavarri-Erasum, B.; Puente, A.; García, A.; García, A.; Bárcena, J.F.; Álvarez, C.; García-Castillo, G. Differential distribution pattern of native *Ruditapes decussatus* and introduced *Ruditapes phillippinarum* clam populations in the Bay of Santander (Gulf of Biscay): Considerations for fisheries management. *Ocean Coast. Manag.* **2012**, *69*, 316–326. [CrossRef]
56. Gómez, G. *Guía de los Moluscos Marinos de Huelva y del Golfo de Cádiz*; Diputación de Huelva: Huelva, Spain, 2017.
57. Orlando, V.E. Presenza nella Sicilia sud-orientale di *Eastonia rugosa* (Helbling, 1779) (Mollusca Bivalvia). *Il Nat. Sicil.* **1979**, *3*, 39–44.
58. Doneddu, M.; Albano, P.G. First record of *Eastonia rugosa* in the Gulf of Olbia, north-eastern Sardinia, Italy. *Mar. Biodivers. Rec.* **2012**, *5*, e89. [CrossRef]
59. Sala-Mirete, A.; Marcos, C.; Vicente-Ríos, M.; Sánchez-Fernández, O.; Texier, J.; Pérez-Ruzafa, A. Changes in macrozoobenthic assemblages of a coastal lagoon in the context of long-term human pressures and a eutrophication process. *Mar. Environ. Res.* **2025**, *208*, 107145. [CrossRef] [PubMed]
60. Pallary, P. Catalogue des mollusques du littoral méditerranéen de l'Egypte. *Mém. Inst. Egypte* **1912**, *7*, 69–207.
61. Taylor, J.D. Feeding ecology of some common intertidal neogastropods at Djerba, Tunisia. *Vie Milieu* **1987**, *37*, 13–20.
62. Pavon, D.; Bertrand, A. Liste commentée des mollusques continentaux du département des Bouches–du–Rhône. *Bull. Soc. Linn. Provence* **2005**, *56*, 35–47.
63. Telesca, L.; Belluscio, A.; Criscoli, A.; Ardizzone, G.; Apostolaki, G.; Fraschetti, S.; Gristina, M.; Knittweis, L.; Martin, C.S.; Pergent, G.; et al. Seagrass meadows *(Posidonia oceanica*) distribution and trajectories of change. *Sci. Rep.* **2015**, *5*, 12505. [CrossRef] [PubMed]
64. Pascual, A.; Martínez, B.; Rodríguez Lázaro, J. Asociaciones de foraminíferos bentónicos en los sedimentos recientes del estuario de Tina Mayor (Asturias, Cantabria). *Geogaceta* **2010**, *48*, 95–98.
65. Consorti, L.; Sabbatino, M.; Parente, M. Insights on the paleoecology of *Ammonia* (Foraminifera, Rotalioidea) from Miocene carbonates of central and southern Apennines (Italy). *Palaeogeogr. Palaeoclimatol. Palaeoecol.* **2021**, *562*, 110105. [CrossRef]
66. Murray, J.W. *Ecology and Applications of Benthic Foraminifera*; Cambridge University Press: Cambridge, UK, 2006.
67. Cheng, J.; Collins, L.S.; Holmes, C. Four thousand years of hábitat change in Florida Bay, as indicated by benthic foraminífera. *J. Foram. Res.* **2012**, *42*, 3–17. [CrossRef]
68. Pint, A.; Frenzel, P. Ostracod fauna associated with *Cyprideis torosa*—An overview. *J. Micropal.* **2017**, *36*, 113–119.
69. Yassini, I. Ecologie des associations d'ostracodes du Bassin d'Arcachon et du littoral Atlantique: Application à l'interpretation de quelques populations du Tertiaire Aquitain. *Bull. Inst. Geol. Bassin Aquitaine* **1969**, *7*, 1–288.
70. Martín-Rubio, M.; Elorza-Remón, M.; Rodríguez-Lázaro, J.; Pascual, A. Distribución areal y ecología de las asociaciones de ostrácodos en la marisma Joyel (Cantabria). *Geogaceta* **2006**, *40*, 187–190.
71. Breman, B. The Distribution of Ostracodes in the Bottom Sediments of the Adriatic Sea. Ph.D. Thesis, Vrije Universiteit, Amsterdam, The Netherlands, 1976.
72. Giraudi, C. Evoluzione tardo-olocenica del delta del Tevere. *Alp. Mediterran. Quat.* **2004**, *17*, 477–482.
73. Lisé-Pronovost, A.; Salomon, F.; Goiran, J.P.; St-Onge, G.; Herries, A.I.R.; Montero-Serrano, J.C.; Heslop, D.; Roberts, A.P.; Levchenko, V.; Zawadzki, A.; et al. Dredging and canal gate technologies in Portus, the ancient harbour of Rome, reconstructed from event stratigraphy and multi-proxy sediment analysis. *Quat. Int.* **2019**, *511*, 78–93. [CrossRef]
74. Goiran, J.P.; Tronchère, H.; Salomon, F.; Carbonel, P.; Djerbi, H.; Ognard, C. Palaeoenvironmental reconstruction of the ancient harbors of Rome: Claudius and Trajan's marine harbors on the Tiber delta. *Quat. Int.* **2010**, *216*, 3–13. [CrossRef]

Disclaimer/Publisher's Note: The statements, opinions and data contained in all publications are solely those of the individual author(s) and contributor(s) and not of MDPI and/or the editor(s). MDPI and/or the editor(s) disclaim responsibility for any injury to people or property resulting from any ideas, methods, instructions or products referred to in the content.